Study of Rb_2 Long-Range States by High-Resolution Photoassociation Spectroscopy

R. A. Cline, J. D. Miller, and D. J. Heinzen
Department of Physics, The University of Texas, Austin, Texas 78712
(Received 21 December 1993)

We study the states of Rb_2 that lie within 35 cm^{-1} of the $5^2S_{1/2} + 5^2P_{3/2}$ dissociation limit with photoassociation spectroscopy of laser-cooled Rb atoms. We observe the rotationally resolved bound levels of the novel 0_g^- "pure long-range" state, which has an inner turning point beyond 25 bohrs. We also identify levels belonging to 1_g and 0_u^+ states and find that the 0_u^+ levels are broadened by predissociation. With our new method, excited molecular states with a binding energy from less than 0.3 to more than 1000 cm^{-1} can be studied with a resolution better than 0.002 cm^{-1}.

PACS numbers: 32.80.Pj, 33.80.Ps, 34.50.Rk

Cold-atom photoassociation spectroscopy is a new method that is opening up previously unexplored, long-range molecular excited states to investigation [1–4]. Photoassociation is the process $A + B + h\nu \rightarrow AB^*$, in which a colliding pair of atoms A and B absorbs a photon of frequency ν to produce a bound excited molecule AB^*. With laser-cooled atoms, narrow photoassociation resonances occur that are associated with the excitation of specific rovibrational states of AB^* [1–4]. Long-range molecular states can be efficiently excited because the initial collisional state wave functions have large amplitudes at long range. These states are expected to exhibit a variety of interesting behavior related to the recoupling of atomic angular momenta at large atomic separation and to retardation effects [5–10]. Cold-atom photoassociation spectroscopy can provide timely information on the long-range interactions between atoms; this information is necessary to determine the role these interactions play in cold-atom frequency standards, efforts to observe Bose-Einstein condensation, and other cold-atom experiments.

In this paper, we present new results which demonstrate the full potential of photoassociation spectroscopy and observe several new features of excited long-range molecular states. In particular, we study the bound states of $^{85}Rb_2$ that lie within 35 cm^{-1} of the $5^2S_{1/2} + 5^2P_{3/2}$ dissociation limit. We observe for the first time the bound levels of a "pure long-range" molecular state [7–9], which has both inner and outer turning points well outside the range of an ordinary chemical bond. We also observe resolved rotational structure and predissociation broadening of long-range states. From these data, we derive potential parameters and a Landau-Zener curve crossing probability that is important to the understanding of fine structure-changing collisions. Highly resolved individual lines exhibit asymmetric line shapes that reflect the thermal energy distribution of the laser-cooled gas.

Several recent experiments demonstrated some of the basic features of cold-atom photoassociation but were somewhat limited in the range of states that could be explored [2,4]. Lett and co-workers [3] detected Na photoassociation resonances associated with a single electronic state over an energy within 3 cm^{-1} of the Na_2^* dissociation limit. In our previous experiment [4], we detected photoassociation of Rb atoms by monitoring their loss from a far-off resonance optical dipole force trap (FORT) [11]. This loss occurs because the Rb_2^* molecules decay predominately to free states of much higher kinetic energy than the trap depth. A single laser both trapped the atoms and induced photoassociation, and excitation to several electronic states with energies up to 980 cm^{-1} below the Rb_2^* dissociation limit was observed. However, with this single laser technique we were unable to obtain high resolution or to probe states much closer than 100 cm^{-1} to the Rb_2^* dissociation limit.

Our present experiment overcomes these limitations. We again detect photoassociation (PA) of ^{85}Rb atoms by measuring their loss from a FORT [11]. However, we now use one fixed frequency FORT laser beam to trap the atoms and superimpose on the trap a separate, tunable, 1 MHz linewidth PA laser beam to drive the photoassociation resonances. This allows us to tune the PA laser to any desired wavelength and power, while at the same time maintaining a strong trap with a very low loss rate due to effects other than photoassociation. With this technique, we are able to probe most of the Rb_2^* excited states that are optically coupled to the ground state, with a resolution better than 0.002 cm^{-1}, and over a range of binding energies from less than 0.3 to more than 1000 cm^{-1}. Results similar to ours have also been recently obtained in Na [12] and Li [13].

In our experiment, about 10^4 ^{85}Rb atoms are loaded into the FORT, with a temperature of 0.7 ± 0.3 mK. The peak density is somewhat uncertain, and lies between 1×10^{12} and 2×10^{13} cm^{-3} [4,11]. The FORT laser is not accurately known, but is on the order of 1×10^{12} cm^{-3} [4]. It has a power $P = 1.6$ W, a waist $w_0 = 8.5 \pm 1.5$ μm, and is chopped at 200 kHz with a 50% duty cycle, which results in a time-averaged well depth $U_0 = 8 \pm 3$ mK. After the FORT is loaded, we superpose the PA laser beam onto the FORT for a period of 100 ms. During this time the atoms are kept optically pumped into their lower $F = 2$ hyperfine level and the

0031-9007/94/73(5)/632(4)$06.00

PA laser beam is chopped at 200 kHz, alternating with the FORT beam. Thus photoassociation is induced only during the 50% fraction of this 100 ms period, during which the PA laser is on and the FORT laser is off. This alternation eliminates power broadening and shifts of the photoassociation resonances by the trapping laser. After the 100 ms delay, both laser beams are turned off, and the remaining atoms are probed with laser-induced fluorescence. This measurement cycle is repeated for a succession of PA laser frequencies. Dips in the atomic fluorescence occur when the PA laser is tuned to a resonance because fewer atoms remain; for a strong resonance about 40% of the trapped atom are lost. An etalon, a Rb saturated absorption spectrometer, and a wave meter with 30 MHz resolution are used to calibrate the PA laser frequency.

The photoassociation spectrum within 35 cm^{-1} of the $5^2S_{1/2} + 5^2P_{3/2}$ dissociation limit is shown in Fig. 1(a). This limit occurs at $D = 12\,816.603$ cm^{-1} for the $5^2S_{1/2}(F = 2) + 5^2S_{1/2}(F = 2) \rightarrow 5^2S_{1/2}(F = 2) + 5^2P_{3/2}(F = 2)$ hyperfine component [14]. In the figure, the fluorescence intensity after the 100 ms delay is plotted as a function of PA laser frequency, with increasing intensity plotted downward. The PA laser intensity is changed in several discrete steps from 2 kW/cm^2 at the low frequency end of the plot to 1 W/cm^2 at the high frequency end.

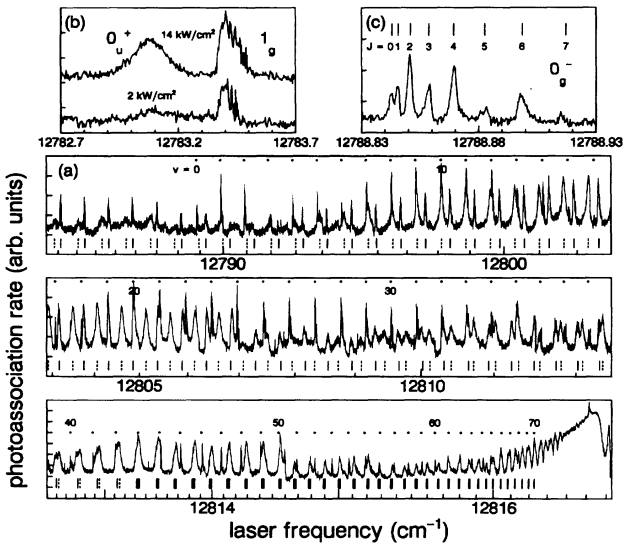

FIG. 1. High-resolution photoassociation spectrum of $^{85}Rb_2$. (a) Complete spectrum over the range within 35 cm^{-1} of the $5^2S_{1/2} + 5^2P_{3/2}$ asymptote. Notice that the frequency scale is expanded as the dissociation limit is approached. Vibrational lines of the 0_g^- pure long-range state are indicated by the dots above the spectrum. Vibrational lines associated with the 0_u^+ and 1_g states are indicated by the dashed and solid lines below the spectrum, respectively. Above 12 813.5 cm^{-1} these two series overlap, as indicated by the thick solid lines. (b) High-resolution scan showing the substructure of the 0_u^+ and 1_g states. The 0_u^+ state exhibits predissociation broadening, whereas the 1_g state displays hyperfine structure. (c) High-resolution scan of the $v = 0$ level of the 0_g^- state, showing a well-resolved rotational series.

Three vibrational series are observed. According to previous calculations [6–10], four long-range attractive potentials connect asymptotically to the $5^2S_{1/2} + 5^2P_{3/2}$ limit and have allowed optical transitions to the Rb_2 ground state (Fig. 2). The 0_u^+ and 1_g potentials connect to strongly bound short-range potentials, whereas the 0_g^- and 1_u are pure long-range states which exhibit a shallow potential well at long range [7–9]. Resolved vibrational levels of the 0_u^+ and 1_g potentials are observed from the low end of the scan to within 0.3 cm^{-1} of the dissociation limit. In addition, we observe the first 70 vibrational levels of the 0_g^- pure long-range state, with $v = 0$ occurring at 12 788.843 ± 0.003 cm^{-1}. We do not detect any 1_u levels, perhaps because its Franck-Condon factors are lower than the other states since it must be excited at shorter range. The vibrational line intensities oscillate, with minima occurring at 12 789 and 12 808.4 cm^{-1} for the 0_u^+ state, at 12 791 and 12 810.0 cm^{-1} for the 1_g state, and at 12 792, 12 802, and 12 812.2 cm^{-1} for the 0_g^- state. These oscillations reflect the structure of the collisional ground state wave function [4]. The last few resolved levels have outer points of $(200–250)a_0$.

Each of the three states shows a distinctive substructure. In Fig. 1(b) we show a high resolution scan over a 0_u^+ and a 1_g vibrational level. The 0_u^+ level is featureless and broad, due to predissociation as discussed below. On the other hand, the 1_g state exhibits hyperfine structure. Its overall width is consistent with a calculated 1.4 GHz hyperfine splitting in the 1_g potential curves [15], together with some additional rotational structure. The 21 most strongly bound 0_g^- vibrational levels exhibit a simple rotational spectrum, as shown for the $v = 0$ level in Fig. 1(c). For $v > 20$ a more complex structure is observed. The rotational spectrum is cut off at $J = 7$, be-

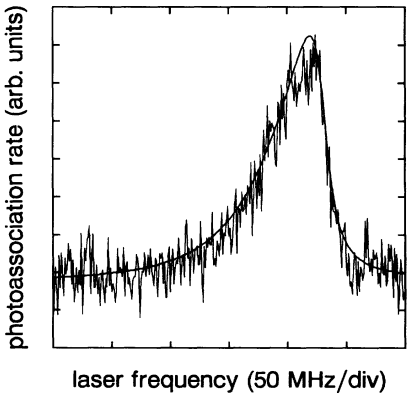

FIG. 2. Approximate potential energy curves for long-range Rb_2 attractive states that connect to the $5^2S_{1/2} + 5^2P_{3/2}$ asymptote and have optically allowed transitions to the Rb_2 ground state.

cause at these energies photoassociation occurs inside the ground state centrifugal barrier at $(100-150)a_0$, so that higher angular momentum states are excluded.

We have determined spectroscopic constants for the low lying 0_g^- levels. We find that $B_e = (1.35 \pm 0.05) \times 10^{-3}$ cm^{-1} and $\alpha_e = (23 \pm 2) \times 10^{-6}$ cm^{-1}, where $E_J = B_v J(J+1)$ are the rotational energies, with $B_v = B_e - \alpha_e(v + \frac{1}{2})$. The quoted error is a systematic uncertainty that results from our inability to accurately model the rotational line shapes. We also find that the 0_g^- well depth (relative to D) is $D_e = 28.295 \pm 0.003$ cm^{-1} and that the $0_g^-(v, J = 0)$ vibrational energies are described by the constants $\omega_e = 1.0770 \pm 0.0001$ cm^{-1} and $\omega_e x_e = (14.31 \pm 0.02) \times 10^{-3}$ cm^{-1}. The calculations of Bussery and Aubert-Frécon [9] give $B_e = 1.166 \times 10^{-3}$ cm^{-1}. Their calculated vibrational level energies yield $D_e = 28.300$ cm^{-1} and $\omega_e = 1.039$ cm^{-1} when they are fitted in the same manner as the data. The discrepancies arise mostly from their use of theoretical rather than experimental atomic oscillator strengths.

The 1_g and 0_u^+ long-range potentials are approximately given by a $-C_3/R^3$ resonant dipole interaction [5–10]. This leads to vibrational level energies near the dissociation limit of $E_v = -(\alpha/C_3^2)(v_D - v)^6 + D$, where v_D is the vibrational defect and α is a known constant [3,16]. We find by fitting our data by this function that $C_3(0_u^+) = 14.64 \pm 0.01 \pm 0.7$ a.u. and $C_3(1_g) = 14.29 \pm 0.02 \pm 0.7$ a.u., where the first uncertainty is statistical and the second systematic. The systematic uncertainty arises because several effects cause a deviation from the above expressions for the potential and for E_v. These include rotational and hyperfine structure, changes in the form of the potential when C_3/R^3 is comparable to the 238 cm^{-1} atomic fine structure splitting [6], and the effect of the short-range part of the potential. The C_3 coefficients can be related to the Rb $5^2P_{3/2}$ atomic excited state lifetime τ_A through $C_3(0_u^+) = (5/3)d^2$ and $C_3(1_g) = [(7^{1/2} + 2)/3]d^2$, where $d^2 = 3\hbar/4k^3\tau_A$, with $k = 80\,529$ cm^{-1} [10]. Using $\tau_A = 26.4 \pm 0.3$ ns [17], we therefore expect that $C_3(0_u^+) = 14.8 \pm 0.2$ a.u. and $C_3(1_g) = 13.8 \pm 0.2$ a.u., in agreement with our derived values. With a complete analysis that more precisely models the potentials and level energies, it should be possible to obtain measurements of C_3 and of τ_A with better than 1% accuracy.

The 0_u^+ levels are broadened by predissociation to the $5^2S_{1/2} + 5^2P_{1/2}$ asymptote, which occurs by spin-orbit mixing of the 0_u^+ components of the $A\,^1\Sigma_u^+$ and $b\,^3\Pi_u$ states at short range [10]. This process also determines the rate of fine structure changing collisions that limit lifetimes and densities in atom traps [10,18]. The level width is $\tau^{-1} = (\Delta E_{v,v-1}/h)P$, where $\Delta E_{v,v-1}$ is the local vibrational splitting and P is the probability of a Landau-Zener transition to the potential asymptotic to $5^2S_{1/2} + 5^2P_{1/2}$ separated atoms during one vibrational oscillation period [10]. From our data, we obtain $P = 0.14 \pm 0.02$, with no significant dependence on v over the energy range from 12 781 to 12 805 cm^{-1}. P cannot be calculated precisely due to its sensitivity to poorly known Rb_2 potentials [15]; a previous theoretical estimate gave $P = 0.36$ [10].

When we examine a single rotational line with very high resolution, we observe asymmetric line shapes like that shown in Fig. 3 for the $J = 3$ level of the vibrational line 12 368 cm^{-1} [4]. The red tail is basically due to the Maxwell-Boltzmann distribution of collision energies [1,19]. The shapes and heights of these rotational lines can provide detailed information on the ground state potentials and the temperature of the laser-cooled gas [19].

In conclusion, we have studied the $^{85}Rb_2$ 0_g^-, 0_u^+, and 1_g long-range states from 35 to 0.3 cm^{-1} below the $5^2S_{1/2} + 5^2P_{3/2}$ asymptote with photoassociation spectroscopy. These studies have yielded the first observations of the bound levels of a pure long-range molecule, of resolved rotational structure in photoassociation spectroscopy, of asymmetric photoassociation line shapes reflecting the thermal energy distribution of the ultracold gas, and of predissociation broadening of photoassociation resonance (similar results are reported in Refs. [12] and [13]). A detailed analysis of the data, in progress, should also provide the Rb-Rb ground state scattering length; knowledge of this parameter is crucial to efforts to observe Bose-Einstein condensation in this system [20]. As shown in Fig. 3, we have also obtained 0.002 cm^{-1} wide photoassociation resonances in the 100–1000 cm^{-1} range of binding energies. Thus, with our technique it should be possible to study a majority of the bound levels of an excited molecule AB^* in the energy range from 0.3 to more than 1000 cm^{-1} below the dissociation limit, with better than 0.002 cm^{-1} resolution, where A and B are any two atoms which can be confirmed in a FORT. With a

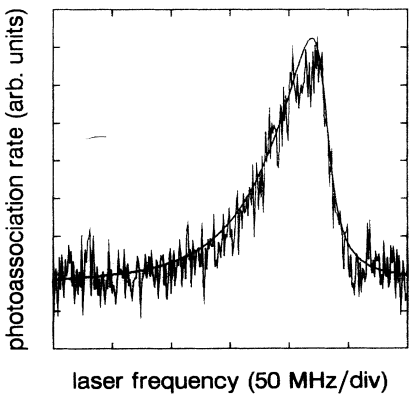

FIG. 3. High-resolution scan over a single rotational line with $J = 3$. The asymmetric line shape reflects the distribution of initial collisional state energies. The solid curve is the convolution of a Lorentzian of width 18 MHz with an exponential of width 40 MHz.

more complete spectrum and analysis, it should be possible to completely characterize the long-range states of the excited molecule and to derive accurate potentials and atomic parameters including lifetimes. We are currently pursuing this goal for Rb_2 and Cs_2.

We thank Paul Julienne, Carl Williams, J. Weiner, Paul Lett, Bill Phillips, and Boudewijn Verhaar for helpful discussions. We thank Mike Matthews and Dian-Jin Han for assistance with the experiment. We gratefully acknowledge the support of the A. P. Sloan Foundation, the R. A. Welch Foundation, and the National Science Foundation.

[1] H. R. Thorsheim, J. Weiner, and P. S. Julienne, Phys. Rev. Lett. **58**, 2420 (1987).
[2] V. Bagnato *et al.*, Phys. Rev. Lett. **70**, 3225 (1993).
[3] P. D. Lett *et al.*, Phys. Rev. Lett. **71**, 2200 (1993).
[4] J. D. Miller, R. A. Cline, and D. J. Heinzen, Phys. Rev. Lett. **71**, 2204 (1993).
[5] W. C. Stwalley, Contemp. Phys. **19**, 65 (1978).
[6] M. Movre and J. Pichler, J. Phys. B **10**, 2631 (1977).
[7] W. C. Stwalley, Y. H. Uang, and G. Pichler, Phys. Rev. Lett. **41**, 1164 (1978).
[8] B. Bussery and M. Aubert-Frécon, J. Chem. Phys. **82**, 3224 (1985).
[9] B. Bussery and M. Aubert-Frécon, J. Mol. Spectrosc. **113**, 21 (1985).
[10] P. S. Julienne and J. Vigué, Phys. Rev. A **44**, 4464 (1991).
[11] J. D. Miller, R. A. Cline, and D. J. Heinzen, Phys. Rev. A **47**, R4567 (1993).
[12] L. P. Ratliff, M. E. Wagshul, P. D. Lett, S. L. Rolston, and W. D. Phillips, J. Chem. Phys. (to be published).
[13] W.I. McAlexander, E.R.I. Abraham, N.W.M. Ritchie, C.J. Williams, H.T.C. Stoof, and R.G. Hulet (to be published).
[14] G. P. Barwood, P. Gill, and W. R. C. Rowley, Appl. Phys. B **53**, 142 (1991).
[15] C. Williams and P. S. Julienne (private communication).
[16] R. J. Leroy and R. B. Bernstein, J. Chem. Phys. **52**, 3869 (1970); W. C. Stwalley, Chem. Phys. Lett. **6**, 241 (1970).
[17] J. K. Link, J. Opt. Soc. Am. **56**, 1195 (1966); R. W. Schmieder *et al.*, Phys. Rev. A **2**, 1216 (1970); S. Svanberg, Phys. Scr. **4**, 269 (1971).
[18] A. Gallagher and D. E. Pritchard, Phys. Rev. Lett. **63**, 957 (1989); D. Sesko *et al.*, Phys. Rev. Lett. **63**, 961 (1989); D. Hoffmann et al., Phys. Rev. Lett. **69**, 753 (1992); C. D. Wallace *et al.*, Phys. Rev. Lett. **69**, 897 (1992); .
[19] R. Napolitano, J. Weiner, C. J. Williams, and P. S. Julienne (to be published).
[20] E. Tiesinga *et al.*, Phys. Rev. A **46**, R1167 (1992).